Carbon isotopic evolution of the terminal Neoproterozoic and early Cambrian: Evidence from the Yangtze Platform, South China

Qingjun Guo [a,b,*], Harald Strauss [b], Congqiang Liu [a], Tatiana Goldberg [b,c],
Maoyan Zhu [d], Daohui Pi [a], Christoph Heubeck [e], Elodie Vernhet [e],
Xinglian Yang [f], Pingqing Fu [a]

[a] *State Key Laboratory of Environmental Geochemistry, Institute of Geochemistry, Chinese Academy of Sciences, Guiyang 550002, China*
[b] *Geologisch-Paläontologisches Institut, Westfälische Wilhelms-Universität Münster, Corrensstrasse 24, 48149 Münster, Germany*
[c] *School of Earth Sciences, James Cook University, Townsville, Queensland 4811, Australia*
[d] *Nanjing Institute of Geology and Palaeontology, Chinese Academy of Sciences, Nanjing 210008, China*
[e] *Institut für Geologische Wissenschaften, Freie Universität Berlin, Malteserstrasse 74-100, D-12249 Berlin, Germany*
[f] *College of Resource and Environment of Guizhou University, Guiyang 550003, China*

Abstract

Profound geotectonic, climatic and biological changes occurred during the terminal Neoproterozoic and its transition into the Early Cambrian. These changes are reflected in temporal variations of the carbon isotopic composition of seawater, recorded in a sedimentary succession on China's Yangtze Platform. However, in addition to secular changes in carbon isotopes, the studied succession reflects additional variations in accordance with the deposition in different sedimentary facies, ranging from shallow water platformal to deeper water basinal settings. Likely a consequence of incorporation of variable amounts of ^{13}C depleted bacterial biomass, this regional signal is superimposed on the secular variations of the global carbon cycle.
© 2007 Elsevier B.V. All rights reserved.

Keywords: Terminal Neoproterozoic; Early Cambrian; Carbon isotopes; Sedimentary facies; Yangtze Platform; South China

1. Introduction

The Neoproterozoic and its transition into the Cambrian is one of the most remarkable time interval in Earth history, spanning major changes in continental configu-

ration, global climate, biological evolution, and variations in oceanic and atmospheric chemical compositions (Knoll, 1991; Hoffman et al., 1998; Walter et al., 2000; Des Marais, 2001). Many of these global perturbations are reflected through secular variations in the isotopic compositions of carbon, sulphur, or strontium (e.g. Jacobsen and Kaufman, 1999; Strauss, 2004). At the same time, respective isotope records (C, Sr) with high temporal resolution provide a global chemostratigraphic correlation scheme, particularly for those sections lacking age-diagnostic biostratigraphic markers and/or precise radiometric age determinations (e.g. Knoll et al., 1986; Knoll,

1991; Knoll, 1992; Kaufman and Knoll, 1995; Shen et al., 1998; Hayes et al., 1999; Walter et al., 2000; Knoll, 2000; Shen and Schidlowski, 2000; Shen et al., 2000; Guo et al., 2003; Jiang et al., 2003a,b; Kirschvink and Raub, 2003; Shields et al., 2004; Condon et al., 2005; Shen et al., 2005). Moreover, paired carbonate and organic carbon isotope records provide an additional proxy ($\Delta\delta_{\text{org-carb}} = \delta^{13}C_{\text{carb}} - \delta^{13}C_{\text{org}}$) for interpreting changes of the global carbon cycle through time, e.g. resulting from changes in atmospheric pCO$_2$ (Kump and Arthur, 1999).

China's Yangtze Platform contains a sedimentary succession of terminal Neoproterozoic and Early Cambrian age, reflecting the deposition in different paleo-environmental settings including inner shelf, outer shelf, slope and basin deposits (e.g. Li et al., 1999a,b; Steiner et al., 2001; Jiang et al., 2003a,b; Shen et al., 2005). These are well exposed in several sections providing a NW–SE profile from the interior platform into the basin (Fig. 1). Resting on diamictites of the Nantuo Formation, the entire sedimentary succession comprises, in ascending stratigraphic order: calcareous sediments, cherts, black shales, and phosphorites of the Neoproterozoic Doushantuo and Dengying (time equivalent of the Liuchapo Fm.) forma-

tions and black shales of the Lower Cambrian Niutitang Formation (time equivalent of the Guojiaba Fm., the Jiumenchong Fm., lower part of the Xiaoyanxi Fm.). Hence, this succession offers a unique opportunity to study the interaction between atmosphere, hydrosphere, biosphere and lithosphere during this critical interval in Earth history.

This study extends previously published carbon isotope records from terminal Proterozoic sediments on the Yangtze Platform (e.g. Magaritz et al., 1986; Lambert et al., 1987; Brasier et al., 1990; Brasier, 1990a,b; Ripperdan, 1994; Wang et al., 1996; Zhou et al., 1997; Zhang et al., 1997; Shen et al., 1998; Zhou et al., 1998; Yang et al., 1999; Li et al., 1999a,b; Wu, 2000; Lei et al., 2000; Shen and Schidlowski, 2000; Shen et al., 2000; Shen, 2002; Zhang et al., 2003; Chu et al., 2003; Guo et al., 2003; Jiang et al., 2003a,b; Shields et al., 2004; Macouin et al., 2004; Condon et al., 2005; Shen et al., 2005), either carbonate carbon or organic carbon isotope data, which were largely generated from sections on the carbonate platform.

Here, an organic carbon isotope record through the terminal Neoproterozoic post-glacial and Early Cambrian
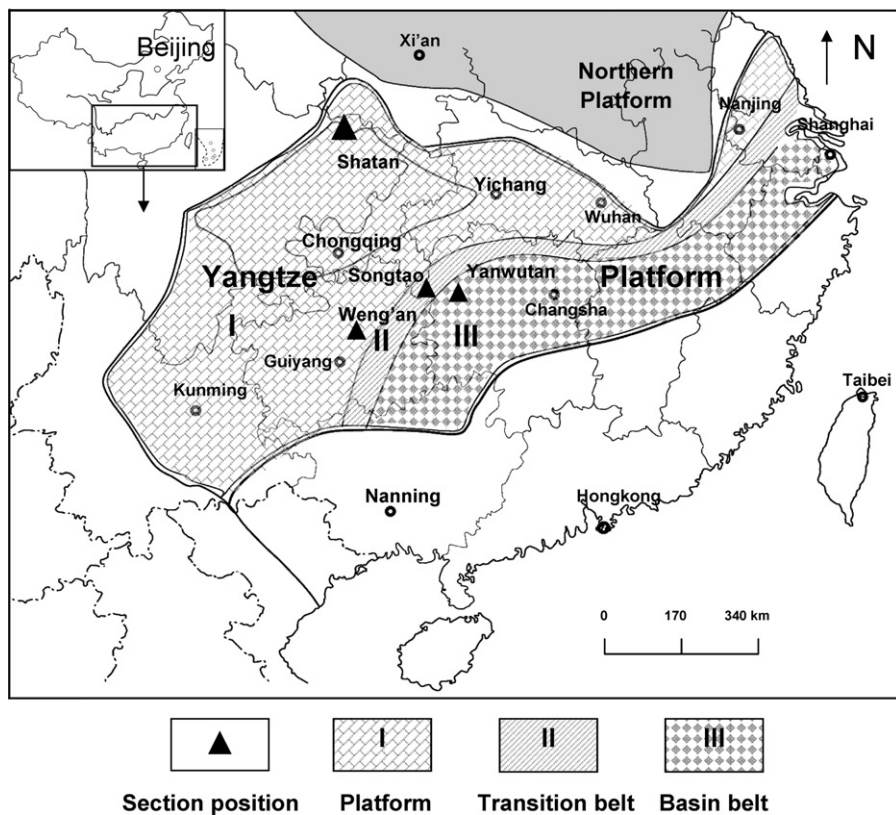

Fig. 1. Geological Map showing the location of (A) Yanwutan–Lijiatuo section, (B) Songtao section, (C) Shatan section and (D) Weng'an section of the Yangtze Platform, South China (modified after Steiner et al., 2001).

stratigraphy is presented, following a profile across the different facies belts. Our systematic investigation documents secular variations in $\delta^{13}C_{org}$ and $\delta^{13}C_{carb}$, which are largely interpreted as perturbations of the global carbon cycle. However, regional effects are superimposed on these isotope records.

2. Geological setting, sections and samples

A succession of lithologically diverse marine sediments was deposited on the Yangtze Platform, South China, during the Precambrian–Cambrian transitional period (Zhu et al., 2003). This sequence of sedimentary rocks was studied at the following locations: the Shatan section (carbonate platform, shelf of northern Yangtze Platform), Shatan County, Sichuan Province, the Weng'an

section (carbonate platform, central part of Yangtze Platform), Weng'an County, Guizhou Province, the Songtao section (transitional belt, Yangtze Platform), Songtao County, Guizhou Province, and the Yanwutan–Lijiatuo section (slope to basin, Yangtze Platform), Yuanling County, Hunan Province (Fig. 1). The base of the studied succession can be constrained in time by the deposition of post-glacial sediments after 635 Ma (Condon et al., 2005). The age of the Precambrian–Cambrian boundary has been dated elsewhere at 544 Ma (Bowring et al., 1993), respectively is placed at 542 Ma (Gradstein et al., 2005). The Lower Cambrian units can be constrained biostratigraphically.

The Shatan section straddles the Precambrian–Cambrian boundary. It comprises the upper part of the Dengying Fm. and the lower part of the Guojiaba Fm.,
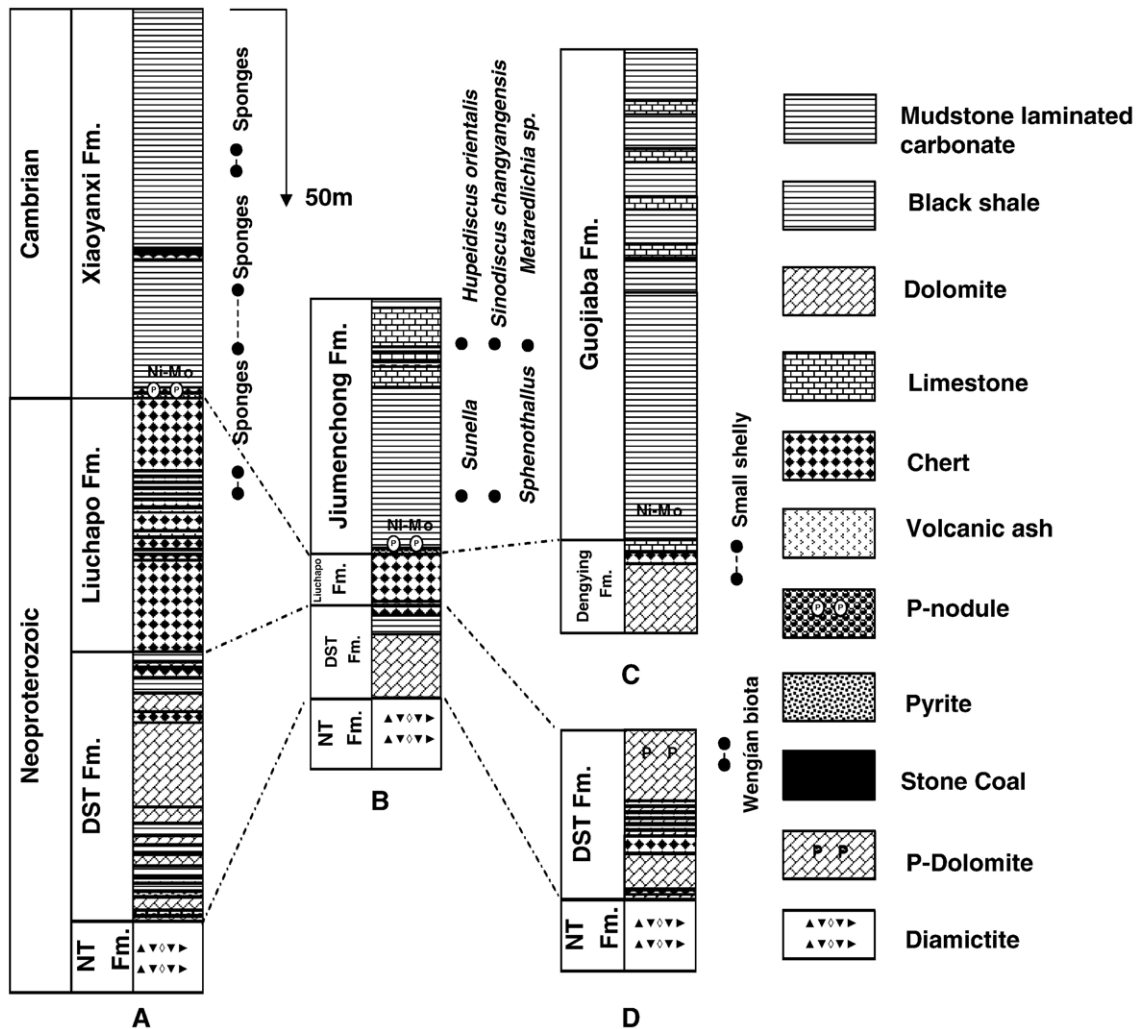

Fig. 2. Lithologs and stratigraphic variations of $\delta^{13}C_{org}$, $\delta^{13}C_{carb}$ and TOC for (A) Yanwutan–Lijiatuo section, (B) Songtao section, (C) Shatan section and (D) Weng'an section and their proposed correlation.

representing shallow water deposition (Fig. 2). Lithologies include light grey carbonates, black shale and siliceous rocks, with abundant small-shelly fossils preserved in the Kuanchuanpu Mbr. of the lowermost Guojiaba Fm. (Steiner et al., 2004). The biostratigraphy of the Shatan section has been well studied (Yang et al., 1983; Yang and He, 1984; He and Yang, 1986; Steiner et al., 2004).

The Weng'an section, also located in a platformal setting, comprises at its base the uppermost siliciclastic portion of the Nantuo glacials and a thick succession of carbonates and phosphorites of the Doushantuo Formation. These rocks contain the exceptionally well-preserved record of multicellular organisms of the Weng'an biota (e.g. Xiao et al., 1998; Li et al., 1998).

On the Yangtze Platform, a transitional belt is located between the proper carbonate platform to the NW and the basinal belt in the SE. The Songtao section is located in this belt and comprises the Doushantuo, the Liuchapo and the Jiumenchong formations, all deposited in a slope environment (Fig. 2). Major lithofacies of the Doushantuo Fm. are bedded, micritic carbonates, and finely laminated black shales. The Liuchapo Fm. consists of black siliceous rocks and phosphatic-siliceous shale and minor limestone concretions. The Jiumenchong Fm. consists of black-grayish carbonaceous shale, limestone and mudstone. The lowermost part of this unit is composed of nodular phosphate rocks. In the black shales of the lower part of the Jiumenchong Fm., bivalved arthropods (*Sunella*) and tubular fossils (*Sphenothallus*) have been reported (at 15 m above the base of the formation) while the upper part consists of limestone with trilobites, including
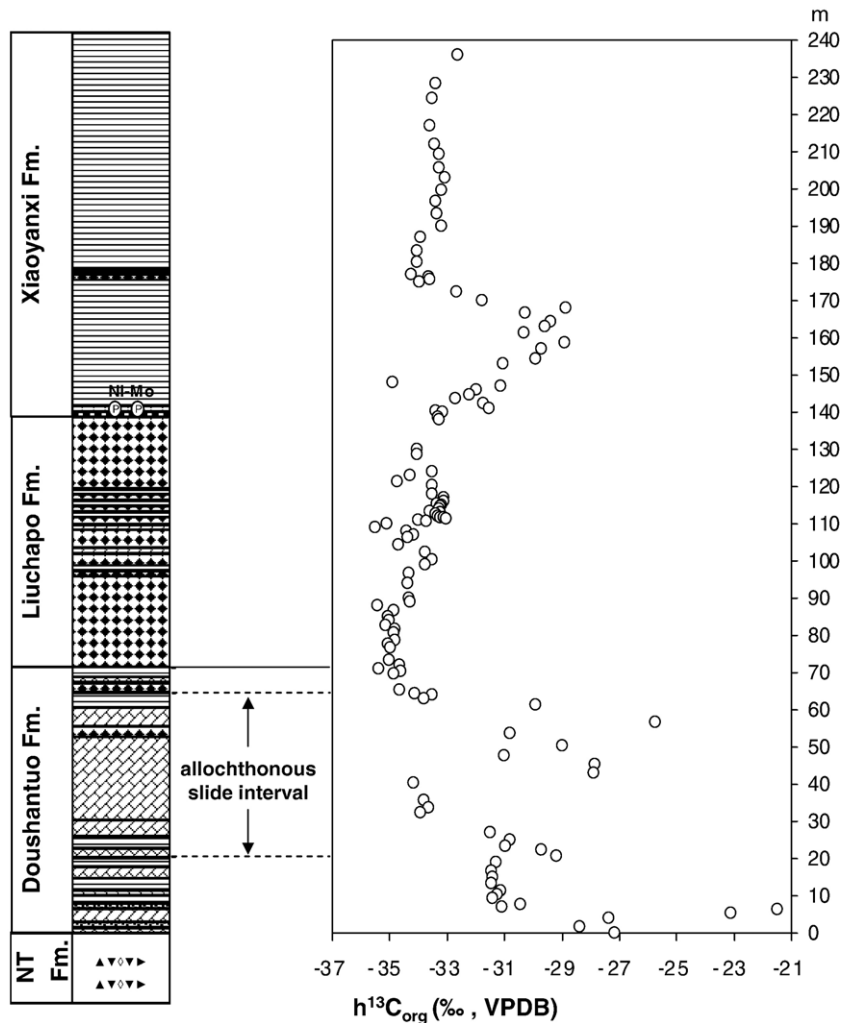

Fig. 3. Stratigraphic variations of $\delta^{13}C_{org}$ for Yanwutan–Lijiatuo section plotted against lithologic column (Key is equal to Figs. 1, 2), with indication of allochthonous interval.

Hupeidiscus orientalis, *Sinodiscus changyangensis* and *Metaredlichia* sp. (Yang et al., 2003).

The basinal belt is mainly situated in the southeastern part of the Yangtze platform. The composite Yanwutan–Lijiatuo section in the Yanwutan area comprises finely laminated shales and silicious rocks (Fig. 2). It is the most complete section studied here, and it includes the Doushantuo (at Yanwutan), the Liuchapo and the Xiaoyanxi (at Lijiatuo) formations, all representing deeper water deposition.

Major lithofacies of the Doushantuo Fm. are bedded, micritic carbonate, mudstone and finely laminated black siliciclastics. However, part of the succession in the Doushantuo Formation represents mass flow deposits from the platform margin into the deeper basin at Yanwutan (Vernhet et al., 2007-this volume). These have been identified between ca. 23 and 65 m above the base of the Doushantuo Formation. Facies and microfacies analysis have shown that basal biolaminated phosphorite micrite

was locally (Luoyixi section, Hunan province) deformed by "tepee" structures resulting of dewaterisation of sediment during emergence periods (Facies 1: Vernhet et al., 2007-this volume). Moreover, high-energy events reworked the phosphorite micrite to form microbreccia (Facies 2: Vernhet et al., 2007-this volume). Furthermore, it appears that basal phosphorites were deposited into a shallow-water protected back-rim lagoon. This lagoon was temporary submitted to emergence periods and to storm waves, which may have passed over the rim. Dolomitised grainstones (Facies 3: Vernhet et al., 2007-this volume) presenting m-scale cross-strata and cm-to-dm-scale crossbedding overlie the basal phosphorites. These coarse-grained sediments characterise shallow subtidal open shelf dominated by waves and currents.

The absence of facies change downslope as well as the absence of a transitional facies between slope shales and phosphorite micrite at the base of the slide sheet and between grainstones and slope shales on the top of the slide
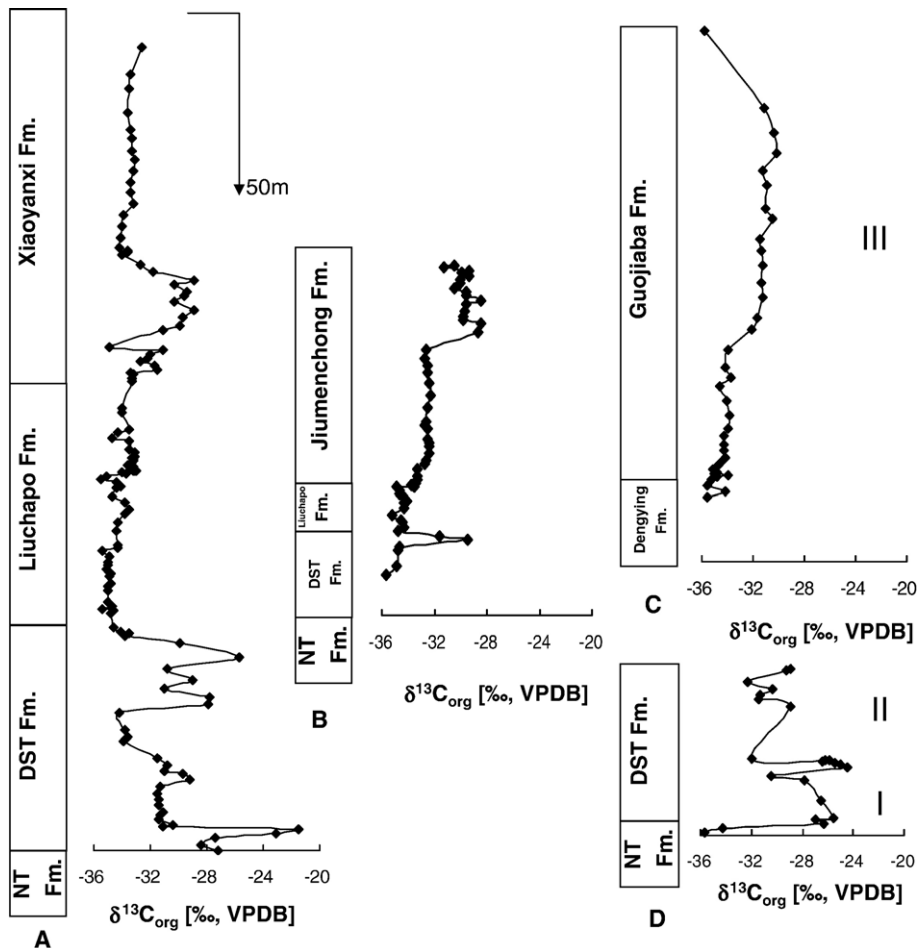

Fig. 4. Stratigraphic variations of $\delta^{13}C_{org}$ for (A)Yanwutan–Lijiatuo section, (B)Songtao section, (C) Shatan section and (D)Weng'an section.

sheet excludes that this sedimentary succession results of platform progradation and retrogradation due to sea level variations. Thus, facies similarity between the shelf and the slide sheet sediments (see correlation scheme in Vernhet et al., 2007-this volume), and the smooth slump fold deformation of these shallow-water facies intervals argue for a platform margin-originated allochthonous slide sheet.

The Liuchapo Fm. consists of black chert and phosphatic-siliceous shale. Fossil sponges were discovered 44 m above the base of the formation. The Xiaoyanxi Fm. consists of cherts and black shale yielding abundant sponges 9 m, 61 m, and between 18 and 23 m above the base of the formation. Again, the bottom layer is composed of nodular phosphate rock.

Table 1
Analytical results for sediments from the Shatan section, Sichuan Province

Sample	Unit Name	Lithology	Depth [m]	$\delta^{13}C_{org}$ [‰, VPDB]	$\delta^{13}C_{carb}$ [‰, VPDB]	$\Delta\delta$ [‰, VPDB]	$\delta^{18}O_{carb}$ [‰, VPDB]	TC [%]	TIC [%]	TOC [%]	H/C
Sat531	Guojiaba Fm.	black shale	154.10	−35.8				5.3	5.0	0.2	0.4
Sat530	Guojiaba Fm.	black shale	131.50	−31.1	0.6	31.7	−13.2		1.2		0.3
Sat529	Guojiaba Fm.	black shale	124.50	−30.4				2.9	2.3	0.6	
Sat528	Guojiaba Fm.	black shale	118.50	−30.1				2.9	2.5	0.4	1.0
Sat527	Guojiaba Fm.	black shale	113.50	−31.3	0.1	31.3	−12.0		2.0		
Sat526	Guojiaba Fm.	black shale	109.00	−30.9							
Sat525	Guojiaba Fm.	black shale	102.40	−31.1	0.4	31.5	−11.8	2.5	1.9	0.6	
Sat524	Guojiaba Fm.	black shale	99.40	−30.5				1.8	1.1	0.7	1.0
Sat523	Guojiaba Fm.	black shale	93.50	−31.5				2.9	2.1	0.8	
Sat522	Guojiaba Fm.	black shale	90.00	−31.4				2.2	1.6	0.6	
Sat521	Guojiaba Fm.	black shale	86.10	−31.3	−0.5	30.8	−13.1	2.5	1.6	0.9	1.1
Sat520	Guojiaba Fm.	black shale	80.80	−31.4	−0.6	30.8	−13.5	2.9	2.1	0.8	
Sat519	Guojiaba Fm.	black shale	76.50	−31.2				2.7	1.6	1.1	0.5
Sat518	Guojiaba Fm.	black shale	70.70	−31.7	−1.4	30.3	−12.5	2.3	1.0	1.3	
Sat517	Guojiaba Fm.	black shale	67.10	−32.1				3.0	1.4	1.6	
Sat516	Guojiaba Fm.	black shale	61.50	−33.9	−2.5	31.4	−12.7	2.1	0.3	1.7	0.8
Sat515	Guojiaba Fm.	black shale	56.30	−34.2				2.7	0.8	1.9	
Sat514	Guojiaba Fm.	black shale	53.50	−33.7							0.8
Sat513	Guojiaba Fm.	black shale	50.90	−34.6				3.3	0.2	3.2	
Sat512	Guojiaba Fm.	black shale	46.40	−34.0	−2.4	31.6	−12.6	4.4	0.5	3.9	
Sat511	Guojiaba Fm.	black shale	42.40	−33.8				3.6	0.4	3.2	0.8
Sat510	Guojiaba Fm.	black shale	38.40	−34.0	−2.4	31.6	−12.7	4.7	0.7	4.1	
Sat509	Guojiaba Fm.	black shale	36.40	−34.2				3.4	0.3	3.1	
Sat508	Guojiaba Fm.	black shale	34.00	−34.3	−2.9	31.4	−11.8	3.7	0.4	3.4	0.6
Sat507	Guojiaba Fm.	black shale	32.00	−34.3	−2.9	31.4	−12.2	4.0	0.3	3.7	
Sat506	Guojiaba Fm.	black shale	30.00	−34.1				4.9	0.0	4.9	
Sat505	Guojiaba Fm.	black shale	28.70	−34.5	−1.7	32.9	−10.4	4.9	0.7	4.2	0.7
Sat504	Guojiaba Fm.	black shale	27.60	−34.8	−2.4	32.4	−10.5	3.5	0.3	3.1	
Sat503	Guojiaba Fm.	black shale	26.80	−35.1	−2.7	32.4	−9.9	2.8	0.3	2.6	0.9
Sat502	Guojiaba Fm.	black shale	25.80	−34.8	−2.5	32.3	−10.2	1.1	0.3	0.9	
Sat501	Guojiaba Fm.	black shale	25.25	−35.0							
Sat500	Guojiaba Fm.	black shale	25.05	−34.0	−3.5	30.5	−12.6				0.5
Sat533	Dengying Fm.	limestone	24.55	−34.8	−0.9	33.9	−12.7	12.4	11.7	0.7	
Sat534	Dengying Fm.	limestone	23.55	−35.3	−1.0	34.3	−11.3	14.7	11.3	3.4	
Sat535	Dengying Fm.	limestone	21.95	−35.5	−1.6	34.0	−8.2				0.4
Sat536	Dengying Fm.	dolostone	20.45	−34.1	−1.4	32.7	−6.7	12.1	12.1	0.0	0.4
Sat537	Dengying Fm.	dolostone	18.85		−0.7		−8.9	12.8	12.3	0.5	
Sat538	Dengying Fm.	dolostone	18.65	−35.6	−1.0	34.6	−9.5				0.4
Sat539	Dengying Fm.	dolostone	17.85		−2.3		−8.6	13.0	12.5	0.5	
Sat540	Dengying Fm.	dolostone	16.05		0.1		−6.4	13.1	12.8	0.4	
Sat541	Dengying Fm.	dolostone	13.65		0.6		−6.1	9.9	9.4	0.5	
Sat542	Dengying Fm.	dolostone	10.85		−0.4		−4.4	13.0	12.7	0.3	
Sat543	Dengying Fm.	dolostone	9.35		−0.3		−4.5	9.0	8.7	0.3	
Sat544	Dengying Fm.	dolostone	7.05		0.0		−4.8	8.9	8.5	0.3	
Sat545	Dengying Fm.	dolostone	3.30		0.0		−4.9	11.3	10.9	0.4	
Sat546	Dengying Fm.	dolostone	0.00		0.0		−4.9	7.2	7.2	0.0	

3. Samples and analytical methods

280 unweathered samples of carbonate, black shale, phosphorite, chert and mudstone were collected for geochemical studies. The stratigraphic positions for the samples are provided in Figs. 3 and 4 and Tables 1–4.

Prior to geochemical analyses, all samples were chipped and pulverized (200 mesh). Subsequently, total-inorganic and organic carbon abundances were determined and isotopic analyses were performed on the total organic and, where applicable, carbonate fractions. For carbonate samples, elemental abundances of Mn, Sr, Fe, Ca and Mg were measured.

3.1. Organic matter

Total organic carbon (TOC) concentrations were determined gravimetrically, following the removal of carbonate with 15% HCl. Organic carbon isotopic compositions were measured for the kerogen fraction. Kerogen extrac-

tion has been performed according to a procedure modified after Lewan (1986) and Fu and Qin (1995). Kerogen preservation was assessed by its H/C atomic ratio, following the determination of C, H elemental abundances.

Organic carbon abundances (TOC) were further determined as the difference between the total carbon (TC) and the total inorganic carbon (TIC) measured with a carbon-sulphur-analyzer (CS-MAT 5500) at the Geologisch-Paläontologisches Institut, Westfälische Wilhelms- Universität Münster, Germany.

Organic carbon isotopic composition ($\delta^{13}C_{org}$) was measured via sealed quartz tube combustion (e.g. Strauss et al., 1992c) and subsequent mass spectrometric analysisat the Geologisch- Paläontologisches Institut, Westfälische Wilhelms- Universität Münster, Münster, Germany.

3.2. Carbonate

CO_2 was liberated from whole rock samples via phosphorylation (McCrea, 1950; Zhen et al., 1986) with

Table 2

Analytical results for sediments from the Weng'an section, Guizhou Province

Sample	Unit Name	Lithology	Depth [m]	$\delta^{13}C_{org}$ [‰, VPDB]	$\delta^{13}C_{carb}$ [‰, VPDB]	$\Delta\delta$ [‰, VPDB]	$\delta^{18}O_{carb}$ [‰, VPDB]	TC [%]	TIC [%]	TOC [%]	H/C
Wen528	Doushantuo Fm.	P-dolostone	47.67	−29.0	−0.2	28.8	−5.2	2.29	2.13	0.15	0.8
Wen527	Doushantuo Fm.	P-dolostone	46.97	−29.2	2.3	31.5	−1.3	9.48	9.34	0.14	0.7
Wen526	Doushantuo Fm.	P-dolostone	46.17		2.6		−1.2				
Wen529	Doushantuo Fm.	P-dolostone	43.67	−32.3	2.1	34.3	−1.6	7.30	6.85	0.45	0.5
Wen530	Doushantuo Fm.	P-dolostone	41.67	−30.4	0.6	30.9	−3.0	5.33	4.93	0.41	0.9
Wen531	Doushantuo Fm.	P-dolostone	39.97	−31.3	−3.2	28.1	−11.4	0.36	0.42		0.5
Wen532	Doushantuo Fm.	P-dolostone	38.97	−31.4	−3.4	28.0	−10.6	0.46	0.42	0.04	
Wen533	Doushantuo Fm.	chert	37.47								
Wen534	Doushantuo Fm.	dolostone	36.67	−28.9	3.6	32.5	−1.3	11.07	10.69	0.38	0.6
Wen525	Doushantuo Fm.	chert	22.07	−32.0	−0.4	31.6	−4.3	2.87	2.42	0.45	
Wen524	Doushantuo Fm.	dolostone	21.67	−25.8	−1.2	24.6	−3.7	11.54	11.27	0.27	0.7
Wen523	Doushantuo Fm.	dolostone	21.37	−26.2	−1.0	25.2	−4.4				0.8
Wen522-1	Doushantuo Fm.	chert	20.97	−26.5	−1.4	25.1	−4.7	2.57	2.31	0.26	
Wen522	Doushantuo Fm.	chert	20.59	−25.5	−1.1	24.4	−4.8	4.82	4.48	0.34	
Wen521	Doushantuo Fm.	chert	20.29	−25.1	−1.5	23.6	−6.8	0.63	0.47	0.16	
Wen520	Doushantuo Fm.	chert	19.47	−24.5	−0.1	24.4	−3.9	3.49	3.20	0.29	
Wen519	Doushantuo Fm.	chert	17.15	−30.5	−3.5	27.0	−10.1	0.47	0.49		0.6
Wen518	Doushantuo Fm.	chert	16.75		−0.7		−4.1				
Wen516	Doushantuo Fm.	Mn-dolostone	15.95	−27.8	−2.8	25.0	−7.2				1.1
Wen515	Doushantuo Fm.	dolostone	10.65		−1.3		−5.1				
Wen514	Doushantuo Fm.	Mn-dolostone	9.9	−26.5	−2.1	24.5	−5.4	10.98	9.68	1.30	1.8
Wen513	Doushantuo Fm.	cap dolostone	6.2		−2.6		−7.2				
Wen512-1	Doushantuo Fm.	mudstone	5.2								
Wen512	Doushantuo Fm.	mudstone	5.1	−25.5	−4.9	20.6	−13.8	0.07	0.01	0.07	
Wen511	Doushantuo Fm.	mudstone	5		−2.3		−2.3	0.05	0.00	0.04	
Wen510	Doushantuo Fm.	cherty dolostone	4.8	−27.0	−2.3	24.7	−6.0	11.08	10.88	0.20	1.5
Wen508	Doushantuo Fm.	cap dolostone	4		−2.0		−5.6				
Wen507	Doushantuo Fm.	cap dolostone	3.45	−26.3	−2.3	24.1	−4.6	11.14	10.82	0.32	1.5
Wen504-1	Nantuo Fm.	black shale	2	−34.3				0.25	0.01	0.24	
Wen504	Nantuo Fm.	black shale	1	−35.6				0.37	0.01	0.37	
Wen501	Nantuo Fm.	black shale	0.07					0.31	0.00	0.31	1.8

Table 3
Analytical results for sediments from the Songtao section, Guizhou Province

Sample	Unit Name	Lithology	Depth [m]	$\delta^{13}C_{org}$ [‰, VPDB]	$\delta^{13}C_{carb}$ [‰, VPDB]	$\Delta\delta$ [‰, VPDB]	$\delta^{18}O_{carb}$ [‰, VPDB]	TC [%]	TIC [%]	TOC [%]
Son580	Jiumenchong Fm.	black Shale	104.25	−30.5				3.53	0.004	3.52
Son579	Jiumenchong Fm.	black Shale	103.55	−31.3				3.81	0.73	3.08
Son578	Jiumenchong Fm.	limestone	102.9	−29.4	0.5	29.9	−12.4	11.46	11.29	0.17
Son577	Jiumenchong Fm.	limestone	102.05	−29.9	0.1	30.0	−13.0	11.70	10.21	1.49
Son576	Jiumenchong Fm.	limestone	101.25	−29.3	2.2	31.5	−12.1	10.51	11.20	0.00
Son575	Jiumenchong Fm.	limestone	100.25	−30.0	0.5	30.5	−12.1	9.71	8.09	1.62
Son574	Jiumenchong Fm.	limestone	99.05	−30.0	2.3	32.3	−11.4	11.65	11.33	0.33
Son573	Jiumenchong Fm.	limestone	97.6	−30.5	0.8	31.3	−10.5	7.49	4.10	3.39
Son572	Jiumenchong Fm.	limestone	96.4	−29.6	−1.6	28.0	−11.7	2.80	2.33	0.47
Son571	Jiumenchong Fm.	limestone	95.2	−29.6	−0.2	29.4	−11.2	9.74	8.82	0.93
Son570	Jiumenchong Fm.	muddy limestone	93.7	−28.4	−0.2	28.2	−11.7	9.09	8.92	0.17
Son569	Jiumenchong Fm.	muddy limestone	92.7	−29.6	−0.6	29.0	−11.7	1.60	1.23	0.37
Son568	Jiumenchong Fm.	muddy limestone	90.4	−29.7	0.0	29.7	−11.7	8.09	8.04	0.05
Son567	Jiumenchong Fm.	limestone	88.8	−29.8	0.9	30.7	−11.6	7.24	5.02	2.23
Son566	Jiumenchong Fm.	muddy limestone	88.2	−29.8	1.2	31.0	−11.6	6.87	5.31	1.56
Son565	Jiumenchong Fm.	muddy limestone	87.2	−28.5	0.6	29.1	−11.1	4.88	4.64	0.24
Son564	Jiumenchong Fm.	limestone	84.45	−28.7	0.8	29.5	−11.3	10.44	10.29	0.14
Son563	Jiumenchong Fm.	black Shale	78.95	−32.6				2.28	0.003	2.28
Son562	Jiumenchong Fm.	black Shale	76.35	−32.7				1.83	0.002	1.83
Son561	Jiumenchong Fm.	black Shale	74.35	−32.5				4.20	0.007	
Son560	Jiumenchong Fm.	black Shale	72.05	−32.5				4.51	0.006	4.50
Son559	Jiumenchong Fm.	black Shale	69.05	−32.4				6.00	0.008	
Son558	Jiumenchong Fm.	black Shale	65.55	−32.3				8.53	0.002	8.53
Son557	Jiumenchong Fm.	black Shale	61.55	−32.5				10.11	0.006	10.11
Son556	Jiumenchong Fm.	black Shale	57.55	−32.6				13.78	0.004	13.78
Son555	Jiumenchong Fm.	black Shale	56.55	−32.7				10.28	0.003	10.28
Son554	Jiumenchong Fm.	black Shale	55.45	−32.5				13.53	0.002	13.53
Son553	Jiumenchong Fm.	black Shale	52.45	−32.5						>10
Son552	Jiumenchong Fm.	black Shale	51.35	−32.4						>10
Son551	Jiumenchong Fm.	black Shale	50.15	−32.4						>10
Son550	Jiumenchong Fm.	black Shale	48.05	−32.4						>10
Son549	Jiumenchong Fm.	black Shale	46.05	−32.6						>10
Son548	Jiumenchong Fm.	black Shale	44.85	−32.7						>10
Son547	Jiumenchong Fm.	black Shale	43.25	−33.3						>10
Son546	Jiumenchong Fm.	black Shale	41.55	−33.3						>10
Son545	Jiumenchong Fm.	black Shale	40.1	−33.3						>10
Son544	Jiumenchong Fm.	black Shale	39.1	−33.4						>10
Son543-1	Jiumenchong Fm.	phosphorite nodule	38.7	−33.6						
Son543-2	Jiumenchong Fm.	chert	38.6	−33.7						
Son543	Jiumenchong Fm.	phosphorite nodule	38.5	−33.5				6.97	0.15	6.83
Son522	Liuchapo Fm.	chert	38.3	−34.9						
Son523	Liuchapo Fm.	chert	37.3	−34.7				1.19	0.05	1.14
Son524	Liuchapo Fm.	chert	36.3	−34.7						
Son525	Liuchapo Fm.	chert	35.3	−34.3						
Son526	Liuchapo Fm.	chert	34.3	−34.1						2.24
Son527	Liuchapo Fm.	chert	33.3	−34.3						2.91
Son528	Liuchapo Fm.	chert	31.7	−34.3						0.86
Son529	Liuchapo Fm.	chert	29.9	−35.2						0.81
Son530	Liuchapo Fm.	chert	28.2	−34.5						13.21
Son531	Liuchapo Fm.	cherty mudstone	27.6	−34.4						11.64
Son532	Liuchapo Fm.	cherty mudstone	26	−34.3						3.83
Son509	Doushantuo Fm.	carbonate	25	−34.8	−8.2	26.6	−11.9	11.63	11.44	0.19
Son510	Doushantuo Fm.	chert	23.6	−31.7				5.48	0.002	5.48
Son511	Doushantuo Fm.	cherty shale	22.5	−29.5				10.44	0.002	10.43
Son512	Doushantuo Fm.	black shale	21.5					13.09	0.039	13.06
Son513	Doushantuo Fm.	black shale	20.5	−34.6				11.48	8.77	2.71

Table 3 (*continued*)

Sample	Unit Name	Lithology	Depth [m]	$\delta^{13}C_{org}$ [‰, VPDB]	$\delta^{13}C_{carb}$ [‰, VPDB]	$\Delta\delta$ [‰, VPDB]	$\delta^{18}O_{carb}$ [‰, VPDB]	TC [%]	TIC [%]	TOC [%]
Son514	Doushantuo Fm.	black shale	19.5	−34.8				4.55	0.01	4.54
Son515	Doushantuo Fm.	carbonate	14.5	−34.9				12.05	10.84	1.21
Son516	Doushantuo Fm.	carbonate	13.3		−9.3		−12.5	11.05	10.98	0.07
Son517	Doushantuo Fm.	carbonate	12.3	−35.7	−7.4	28.3	−7.5	10.45	9.16	1.29
Son518	Doushantuo Fm.	carbonate	11.4		−9.2		−12.6	10.87	10.83	0.03
Son519	Doushantuo Fm.	carbonate	9.6		−9.1		−12.6	11.02	10.98	0.04
Son520	Doushantuo Fm.	cap carbonate	8.3		−7.9		−10.6	10.56	10.57	0.00
Son521	Doushantuo Fm.	cap carbonate	7		−9.0		−13.1	10.70		
	Nantuo Fm.	diamictite	0							

enriched H_3PO_4 at 25 °C for 24 h (limestone), 50 °C for 24 h (dolostone), 75 °C for 16 h (dolostone), and 75 °C for 24 h (mudstone) (Wachter and Hayes, 1985; Zhen et al., 1986). All carbonate carbon and oxygen isotopic compositions were measured in the Institute of Geochemistry, Chinese Academy of Sciences, Guiyang, China, using at Finnigan MAT 252 mass spectrometer. The analytical procedure was controlled by measuring the Guiyang laboratory standard GBW 04406 for its $\delta^{13}C_{carb}$ ($\delta^{13}C_{carb-standard}$: − 10.85‰; Standard deviation: 0.05‰) and $\delta^{18}O_{carb}$ ($\delta^{18}O_{carb-standard}$: − 12.40‰; Standard deviation: 0.15‰) values. Results are reported as $\delta^{13}C_{carb}$ and $\delta^{18}O_{carb}$ relative to the Vienna Peedee Belemnite Standard (VPDB). Standard deviation was usually better than ± 0.1 ‰.

In order to constrain carbonate diagenesis, samples were further studied for their elemental abundances of Mn, Sr, Fe, Ca and Mg (Veizer, 1983; Popp et al., 1986; Kaufman et al., 1993; Veizer et al., 1997, 1999). Samples were digested in 3N HCl and elemental concentrations were measured with atomic absorption spectroscopy. Results were corrected for the amount of insoluble residue (soluble (%) = (total weight − weight insoluble residue)/(total weight)).

4. Results

The total organic carbon content (TOC) ranges from <0.1 to 45.9 wt.%. Throughout the entire stratigraphic succession, the organic carbon isotopic composition ($\delta^{13}C_{org}$) displays values between −35.8 and −21.5‰, averaging −32.3 ±2.6‰ ($n=243$). Carbonate carbon isotope data lie between −9.3 and +2.3‰, averaging −2.5±3.3‰ ($n=105$), and respective $\delta^{18}O_{carb}$ values range from −13.8 to −1.2‰, averaging −8.2±3.6‰ ($n=105$). The difference between the organic and carbonate carbon isotopic compositions ($\Delta\delta_{org-carb}=\varepsilon_{TOC}=\delta^{13}C_{carb}-\delta^{13}C_{org}$) varies between 19.4 and 34.6‰, averaging 28.1±4‰ (n=82). Elemental abundances of

Mn, Sr and Fe are highly variable (Mn: 84-8324 ppm; Sr: 44-9391 ppm; Fe: 1153-75593 ppm). Analytical results are given in Tables 1–5.

5. Preservation of the organic matter

Post-depositional processes such as microbial remineralisation and, moreover, thermal alteration have the potential to change the primary isotopic composition of sedimentary organic matter (Claypool and Kaplan, 1974; Irwin et al., 1977; Berner, 1981; Strauss et al., 1992a; Samuelsson and Strauss, 1999). Therefore, it is essential to assess the state of preservation of the sedimentary organic matter prior to interpretation of its organic carbon isotopic composition.

Bacterial degradation of organic matter depends on available oxidants that ultimately result in an ecological succession of bacteria and a frequently depth-stratified series of biogeochemical zones within the sediment. This stratification can be reflected in the preservation of organic matter, and characterized by distinct isotopic signatures which are different from the sedimentary precursor material (i.e., primary production from the photic zone). Post-depositional thermal alteration will ultimately result in the loss of biomarker information as well as ^{13}C depleted constituents of the organic matter (Strauss et al., 1992a; Samuelsson and Strauss, 1999).

From a geochemical point of view, the H/C ratio is an important parameter for estimating the preservation state of kerogen, because H/C ratio decreases with increasing thermal alteration. Independent studies have revealed a direct relationship between the H/C and $\delta^{13}C_{ker}$ values (Hayes et al., 1983; Strauss et al., 1992a,b; Des Marais et al., 1992; Samuelsson and Strauss, 1999). These studies showed that an H/C ratio smaller than 0.2 corresponds to thermally altered kerogen, which likely experienced significant shifts in $\delta^{13}C_{ker}$. These studies revealed that the carbon isotopic composition of

Table 4
Analytical results for sediments from the Yanwutan–Lijiatuo section, Hunan Province

Sample	Unit Name	Lithology	Depth [m]	$\delta^{13}C_{org}$ [‰, VPDB]	$\delta^{13}C_{carb}$ [‰, VPDB]	$\Delta\delta$ [‰, VPDB]	$\delta^{18}O_{carb}$ [‰, VPDB]	TC [%]	TIC [%]	TOC [%]
Ljt593	Xiaoyanxi Fm.	black shale	236.1	−32.6				10.09	0.0004	10.09
Ljt592	Xiaoyanxi Fm.	black shale	228.3	−33.4				3.87	0.0001	3.87
Ljt591	Xiaoyanxi Fm.	black shale	224.2	−33.5				6.93	0.0013	6.93
Ljt590	Xiaoyanxi Fm.	black shale	217.1	−33.6				4.17	0.0004	4.17
Ljt589	Xiaoyanxi Fm.	black shale	212.1	−33.4				6.09	0.0002	6.09
Ljt588	Xiaoyanxi Fm.	black shale	209.4	−33.3				7.00	0.0018	6.99
Ljt587	Xiaoyanxi Fm.	black shale	205.7	−33.3				7.13	0.0048	7.12
Ljt586	Xiaoyanxi Fm.	black shale	203	−33.1				14.32	0.0018	14.32
Ljt585	Xiaoyanxi Fm.	black shale	199.7	−33.2				15.40	0.0007	15.40
Ljt584	Xiaoyanxi Fm.	black shale	196.6	−33.4				13.13	0.0012	13.13
Ljt583	Xiaoyanxi Fm.	black shale	193.4	−33.4				11.37	0.0005	11.37
Ljt582	Xiaoyanxi Fm.	black shale	190.1	−33.2				11.48	0.0013	11.48
Ljt581	Xiaoyanxi Fm.	black shale	187	−33.9				7.47	0.0006	7.47
Ljt580	Xiaoyanxi Fm.	black shale	183.5	−34.0				7.26	0.0002	7.25
Ljt579	Xiaoyanxi Fm.	black shale	180.2	−34.1				9.01	0.0015	9.01
Ljt578	Xiaoyanxi Fm.	black shale	177.1	−34.2				8.51	0.0012	8.51
Ljt577	Xiaoyanxi Fm.	Stone coal	176.3	−33.6				11.10	0.0030	11.10
Ljt576	Xiaoyanxi Fm.	cherty shale	175.8	−33.6				2.06	0.0028	2.06
Ljt575	Xiaoyanxi Fm.	cherty shale	175.05	−34.0				7.39	0.0022	7.39
Ljt574	Xiaoyanxi Fm.	black shale	173.55					17.65	0.0014	17.65
Ljt573	Xiaoyanxi Fm.	black shale	172.25	−32.7				3.57	0.0021	3.57
Ljt572	Xiaoyanxi Fm.	black shale	170.05	−31.8				1.88	0.0021	1.88
Ljt571	Xiaoyanxi Fm.	black shale	167.85	−28.9				0.72	0.0014	0.72
Ljt570	Xiaoyanxi Fm.	black shale	166.55	−30.3				1.47	0.0011	1.47
Ljt569	Xiaoyanxi Fm.	black shale	164.45	−29.4				1.01	0.0007	1.01
Ljt568	Xiaoyanxi Fm.	black shale	163.15	−29.6				1.40	0.0010	1.40
Ljt567	Xiaoyanxi Fm.	black shale	161.45	−30.3						
Ljt566	Xiaoyanxi Fm.	black shale	158.75	−28.9						
Ljt565	Xiaoyanxi Fm.	black shale	156.95	−29.7						
Ljt564	Xiaoyanxi Fm.	black shale	154.45	−29.9				1.42	0.0039	1.42
Ljt563	Xiaoyanxi Fm.	black shale	152.95	−31.1				1.54	0.0004	1.54
Ljt562	Xiaoyanxi Fm.	black shale	147.95	−34.9				2.97	0.0002	2.97
Ljt559	Xiaoyanxi Fm.	black shale	147.05	−31.1				5.55	0.0005	5.55
Ljt558	Xiaoyanxi Fm.	black shale	145.85	−32.0				14.03	0.0008	14.03
Ljt557	Xiaoyanxi Fm.	black shale	144.65	−32.2				14.79	0.0003	14.79
Ljt556	Xiaoyanxi Fm.	black shale	143.65	−32.7				17.04	0.0030	17.03
Ljt555	Xiaoyanxi Fm.	black shale	142.35	−31.7				2.97	0.0021	2.96
Ljt554	Xiaoyanxi Fm.	black shale	141.15	−31.5				1.10	0.0901	1.01
Ljt553	Xiaoyanxi Fm.	black shale	140.35	−33.4				18.69	0.0002	18.69
Ljt552	Xiaoyanxi Fm.	cherty shale	139.85	−33.2				19.16	0.0030	19.15
Ljt551	Xiaoyanxi Fm.	chert	138.75	−33.3				1.92	0.0075	1.91
Ljt550	Xiaoyanxi Fm.	phosphorite nodule	138.15	−33.3				3.42	0.0012	3.42
Ljt549	Liuchapo Fm.	chert	130.15	−34.0				1.55	0.0009	1.55
Ljt548	Liuchapo Fm.	chert	128.65	−34.0				1.99	0.0077	1.99
Ljt547	Liuchapo Fm.	chert	127.25					1.17	0.0003	1.17
Ljt546	Liuchapo Fm.	chert	125.55					2.22	0.0021	2.22
Ljt545	Liuchapo Fm.	carbonacious chert	123.95	−33.5				0.51	0.1030	0.41
Ljt544	Liuchapo Fm.	chert	122.95	−34.3				1.36	0.0026	1.36
Ljt543	Liuchapo Fm.	chert	121.35	−34.7				1.22	0.0072	1.21
Ljt542	Liuchapo Fm.	chert	120.45	−33.5				1.35	0.0008	1.35
Ljt541	Liuchapo Fm.	black shale	119.25					4.97	0.0004	4.97
Ljt541	Liuchapo Fm.	chert	118.05	−33.5				1.55	0.0002	1.55
Ljt540	Liuchapo Fm.	black shale	116.9	−33.1				4.18	0.0006	4.18
Ljt539	Liuchapo Fm.	chert	116	−33.1				2.48	0.0038	2.47
Ljt538	Liuchapo Fm.	black shale	115.2	−33.3				9.00	0.0000	9.00
Ljt537	Liuchapo Fm.	chert	115.15	−33.2				2.05	0.0009	2.05

(continued on next page)

Table 4 (*continued*)

Sample	Unit Name	Lithology	Depth [m]	$\delta^{13}C_{org}$ [‰, VPDB]	$\delta^{13}C_{carb}$ [‰, VPDB]	$\Delta\delta$ [‰, VPDB]	$\delta^{18}O_{carb}$ [‰, VPDB]	TC [%]	TIC [%]	TOC [%]
Ljt536	Liuchapo Fm.	carbonacious chert	114.7	−33.2				6.34	0.0001	6.34
Ljt535	Liuchapo Fm.	carbonacious chert	114.1	−33.3				5.51	0.0003	5.51
Ljt534	Liuchapo Fm.	black shale	113.45	−33.6				13.63	0.0017	13.63
Ljt533	Liuchapo Fm.	chert	113.4					6.42	0.0018	6.42
Ljt532	Liuchapo Fm.	black shale	112.9	−33.2				5.11	0.0010	5.11
Ljt531	Liuchapo Fm.	chert	112.8	−33.4				3.52	0.0004	3.51
Ljt530	Liuchapo Fm.	chert	112.15	−33.3				3.78	0.0020	3.78
Ljt529	Liuchapo Fm.	black shale	112.1	−33.3				6.50	0.0003	6.50
Ljt528	Liuchapo Fm.	black shale	111.8	−33.2				5.73	0.0009	5.73
Ljt527	Liuchapo Fm.	muddy chert	111.55	−33.1				1.95	0.0027	1.95
Ljt526	Liuchapo Fm.	black shale	111.5	−33.0				2.18	0.0022	2.18
Ljt525	Liuchapo Fm.	muddy chert	111.1	−34.0				1.65	0.0040	1.65
Ljt524	Liuchapo Fm.	muddy chert	110.7	−33.7				0.54	0.0013	0.54
Ljt523	Liuchapo Fm.	cherty shale	109.9	−35.1				0.60	0.0008	0.60
Ljt522	Liuchapo Fm.	chert	109	−35.5				0.91	0.0002	0.91
Ljt521	Liuchapo Fm.	cherty lapillus	108.1	−34.4				0.28	0.0025	0.28
Ljt520	Liuchapo Fm.	chert	107.1	−34.1				0.55	0.0013	0.54
Ljt519	Liuchapo Fm.	chert	106.4	−34.4				0.76	0.0004	0.76
Ljt518	Liuchapo Fm.	chert	104.2	−34.7				1.06	0.0038	1.06
Ljt517	Liuchapo Fm.	chert	102.4	−33.8				1.05	0.0010	1.05
Ljt516	Liuchapo Fm.	chert	100.4	−33.5				0.36	0.0030	0.36
Ljt515	Liuchapo Fm.	chert	99.1	−33.8				0.65	0.0002	0.65
Ljt514	Liuchapo Fm.	chert	96.6	−34.3				1.41	0.0023	1.41
Ljt513	Liuchapo Fm.	chert	94.1	−34.4				0.62	0.0010	0.62
Ljt512	Liuchapo Fm.	chert	89.9	−34.3				0.49	0.0028	0.49
Ljt511	Liuchapo Fm.	chert	89	−34.3				0.26	0.0030	0.25
Ljt510	Liuchapo Fm.	chert	88.1	−35.4				1.14	0.0004	1.14
Ljt509	Liuchapo Fm.	chert	86.6	−34.9				0.81	0.0015	0.81
Ljt508	Liuchapo Fm.	chert	85	−35.0				0.94	0.0051	0.93
Ljt507	Liuchapo Fm.	chert	84	−35.0				1.00	0.0045	0.99
Ljt506	Liuchapo Fm.	chert	82.8	−35.1				1.09	0.0005	1.09
Ljt505	Liuchapo Fm.	chert	81.65	−34.8				0.72	0.0030	0.72
Ljt504	Liuchapo Fm.	chert	80.55	−34.9				0.96	0.0005	0.95
Ljt503	Liuchapo Fm.	chert	79.6					1.09	0.0110	1.08
Ljt502	Liuchapo Fm.	chert	78.7	−34.8				0.93	0.0005	0.93
Ljt501	Liuchapo Fm.	chert	77.7	−35.0				0.91	0.0022	0.91
Ljt500	Liuchapo Fm.	chert	76.7	−35.0				1.02	0.0111	1.01
Ljt561	Liuchapo Fm.	chert	73.2	−35.0				1.06	0.0013	1.06
Ljt560	Liuchapo Fm.	chert	72	−34.7				1.10	0.0045	1.09
Yaw543	Doushantuo	black shale	71	−35.4				11.00	0.0095	10.99
Yaw542	Doushantuo	cherty shale	70.5	−34.6				1.15	0.0017	1.15
Yaw541	Doushantuo	black shale	69.8	−34.8				1.16	0.0054	1.15
Yaw540	Doushantuo	carbonaceous chert	65.5	−34.6				1.16	0.0020	1.16
Yaw539	Doushantuo	chert	64.3	−34.1				1.23	0.0003	1.23
Yaw538	Doushantuo	black shale	64	−33.5				3.29	0.0109	3.28
Yaw537	Doushantuo	black shale	63	−33.8				17.94	0.0104	17.93
Yaw536	Doushantuo	black shale	61.2	−29.9				0.18	0.0019	0.18
Yaw535	Doushantuo	cherty dolostone	56.7	−25.7	−6.3	19.4	−11.3	0.34	0.2315	0.10
Yaw534	Doushantuo	chert	53.7	−30.8				0.20	0.0830	0.12
Yaw533	Doushantuo	muddy dolostone	52.1		−8.0		−2.7	12.71	12.242	0.47
Yaw532	Doushantuo	muddy dolostone	50.3	−29.0	−6.3	22.6	−3.1	11.93	11.355	0.58
Yaw531	Doushantuo	muddy dolostone	47.7	−31.0	−6.1	24.9	−3.9	11.89	11.097	0.79
Yaw530	Doushantuo	muddy dolostone	45.2	−27.8	−7.3	20.5	−4.2	11.49	10.747	0.74
Yaw529	Doushantuo	muddy dolostone	43	−27.9	−7.0	20.9	−3.5	12.16	11.646	0.51
Yaw528	Doushantuo	dolostone	40.4	−34.2	−7.2	27.0	−5.6	9.80	8.793	1.00
Yaw527	Doushantuo	muddy dolostone	38.2		−7.0		−3.7	12.15	10.505	1.64
Yaw526	Doushantuo	muddy dolostone	35.6	−33.8	−8.0	25.8	−4.0	12.00	10.130	1.87
Yaw525	Doushantuo	muddy dolostone	33.6	−33.6	−8.4	25.2	−4.5	11.00	8.960	2.04

Table 4 (continued)

Sample	Unit Name	Lithology	Depth [m]	$\delta^{13}C_{org}$ [‰, VPDB]	$\delta^{13}C_{carb}$ [‰, VPDB]	$\Delta\delta$ [‰, VPDB]	$\delta^{18}O_{carb}$ [‰, VPDB]	TC [%]	TIC [%]	TOC [%]
Yaw524	Doushantuo	muddy dolostone	32.3	−33.9	−8.7	25.2	−5.2	11.28	9.041	2.23
Yaw523	Doushantuo	muddy dolostone	29.5		−8.6		−6.7	7.84	6.112	0.83
Yaw522	Doushantuo	dolostone	27	−31.5	−6.9	24.6	−9.4	12.78	11.952	0.83
Yaw521	Doushantuo	organic-rich dolostone	24.9	−30.8	−7.4	23.4	−7.6	11.29	10.117	1.17
Yaw520	Doushantuo	organic-rich dolostone	23.5	−31.0	−8.7	22.3	−7.0	10.01	8.340	1.67
Yaw519	Doushantuo	dolostone	22.5	−29.7	−8.9	20.8	−6.6	11.68	11.496	0.18
Yaw518	Doushantuo	dolostone	20.8	−29.2	−4.3	24.9	−5.8	10.62	10.500	0.12
Yaw517	Doushantuo	organic-rich dolostone	18.9	−31.3	−3.0	28.3	−7.0	9.72	4.654	5.07
Yaw516	Doushantuo	dolostone shale	16.7	−31.5	−3.0	28.5	−7.5	12.38	8.124	4.25
Yaw515	Doushantuo	dolostone shale	15	−31.4	−1.6	29.8	−6.9	11.24	5.930	5.31
Yaw514	Doushantuo	black shale	13.2	−31.4				7.32	0.0080	7.31
Yaw513	Doushantuo	black shale	11.2	−31.1				3.75	0.0024	3.75
Yaw512	Doushantuo	lappilus	11							
Yaw511	Doushantuo	black shale	10.3	−31.3	2.3	33.6	−7.4	3.17	0.0046	3.17
Yaw510	Doushantuo	black shale	9.4	−31.4				3.68	0.0005	3.68
Yaw509	Doushantuo	mudstone	7.7					0.07	0.0094	0.06
Yaw508	Doushantuo	black shale	7.65	−30.4				1.11	0.0002	1.11
Yaw507	Doushantuo	chert	7.05	−31.1	−7.6	23.4	−12.1	0.70	0.3059	0.40
Yaw506	Doushantuo	pyrite layer	7					0.09	0.0182	0.07
Yaw505	Dou-cap	cap dolostone	6.4	−21.5	1.1	22.6	−4.0	11.68	11.307	0.37
Yaw504	Dou-cap	cap dolostone	5.2	−23.1	−1.5	21.6	−4.5	10.98	10.538	0.44
Yaw503	Dou-cap	cap dolostone	3.9	−27.4	−3.6	23.8	−9.2	12.01	11.403	0.60
Yaw502	Dou-cap	pyrite nodule	2.6							
Yaw501	Dou-cap	cap dolostone	1.7	−28.4	−30.6	24.7	−8.7	10.68	10.363	0.32
Yaw500	Dou-cap	cap dolostone	0	−27.2	−4.1	23.0	−10.0	0.91	0.7967	0.11
	Nantuo Fm.									

kerogen displaying an H/C > 0.2 has probably been altered (increased) by less than 3‰ (Hayes et al., 1983). The more severely altered kerogens (H/C < 0.2) are frequently more ^{13}C enriched (Strauss et al., 1992a; Samuelsson and Strauss, 1999).

The H/C ratios of samples obtained for kerogen in this study range between 0.31 and 1.76. The absence of a clear correlation between H/C and $\delta^{13}C_{org}$ is taken as evidence that the carbon isotopic composition of kerogen from this study has not been significantly shifted during post-depositional processes.

6. Carbonate diagenesis

Carbonate diagenesis can obliterate primary depositional trends which reflect seawater chemistry. Overall, an increase in the elemental abundances of Fe and Mn and a decrease in Sr concentration can be observed during diagenesis (e.g. Veizer, 1983; Marshall, 1992). Similarly, progressing diagenetic alteration of carbonates typically leads to a decrease in the isotopic compositions of carbon and oxygen. The former is a consequence of the incorporation of CO_2 derived from the oxidation of organic matter during carbonate

precipitation. The latter is a result of meteoric water alteration.

In order to evaluate the degree of carbonate diagenesis and, thus, the question of whether the observed geochemical signatures reflect near primary signals of deposition or the effects of advanced diagenetic alteration, Kaufman et al. (1993, 1995) have proposed certain threshold levels. A Mn/Sr ratio < 2 and $\delta^{18}O$ values more positive than −10‰ (better even more positive than −5‰) are thought to be consistent with the view, that respective carbonates have retained near primary carbonate carbon isotope values.

Elemental abundances and Mg/Ca and Mn/Sr ratios are quite variable (Table 5). No correlation exists between commonly applied geochemical indicators for carbonate diagenesis, such as Mn/Sr or Mg/Ca and the respective $\delta^{13}C$ and/or $\delta^{18}O$ values (Fig. 5). However, absolute values indicate a significant degree of dolomitization. Furthermore, while many Mn/Sr ratios are below 5, others are substantially higher, attesting to a significant degree of diagenetic alteration.

Elemental abundances and ratios clearly indicate that carbonates have been altered during diagenesis. Hence, we will only cautiously interpret the carbonate carbon

Table 5
Elemental abundances (Ca, Mg, Mn, Sr, Fe) and isotopic compositions of $\delta^{18}O_{carb}$ and $\delta^{13}C_{carb}$ in carbonates from the Yanwutan–Lijiatuo, Shatan, Songtao and Weng'an sections

Sample	Lithology	Soluble residue [%]	Fe [%]	Ca [%]	Mg [%]	Mn [%]	Sr [%]	Mg/Ca	Mn/Sr	$\delta^{13}C_{carb}$ [‰, VPDB]	$\delta^{18}O_{carb}$ [‰, VPDB]
Yaw500	cap dolostone	6.5	7.56	31.70	13.59	0.83	0.0653	0.43	12.75	−4.1	−10
Yaw501	cap dolostone	84.0	0.83	22.22	5.48	0.33	0.0151	0.25	22.17	−3.6	−8.7
Yaw503	cap dolostone	93.0	0.48	22.19	5.14	0.24	0.0100	0.23	23.52	−3.6	−9.2
Yaw505	cap dolostone	93.0	0.56	21.75	5.00	0.24	0.0300	0.23	8.12	1.1	−4
Yaw515	dolomitic shale	47.5	4.49	30.36	7.58	0.12	0.0445	0.25	2.70	−1.6	−6.9
Yaw517	organic dolostone	37.2	6.37	35.80	8.31	0.14	0.0613	0.23	2.26	−3	−7.5
Yaw520	organic dolostone	67.1	2.09	28.58	6.03	0.07	0.0151	0.21	4.93	−8.7	−7
Yaw523	muddy dolostone	48.5	0.82	26.41	8.59	0.10	0.0244	0.33	4.22	−8.6	−6.7
Yaw526	muddy dolostone	82.8	0.48	24.96	5.74	0.04	0.0061	0.23	6.93	−8	−4
Yaw529	muddy dolostone	95.7	0.33	21.65	5.16	0.05	0.0044	0.24	11.64	−7	−3.5
Sat500	phosphorite limestone	93.0	0.23	33.16	0.06	0.11	0.0309	0.00	3.53	−3.5	−12.6
Sat535	limestone	73.0	0.37	16.66	7.19	0.09	0.0104	0.43	8.73	−1.6	−8.2
Sat536	dolostone	97.0	0.12	24.15	10.31	0.14	0.0131	0.43	10.47	−1.4	−6.7
Sat537	dolostone	97.5	0.17	22.09	11.56	0.09	0.0104	0.52	8.47	−0.7	−8.9
Sat538	dolostone	96.0	0.23	21.50	11.73	0.07	0.0106	0.55	6.31	−1	−9.5
Wen507	cap dolostone	88.0	0.95	21.83	12.55	0.24	0.0077	0.58	31.18	−2.3	−4.6
Wen510	cherty dolostone	89.0	0.60	20.97	12.10	0.13	0.0076	0.58	17.32	−2.3	−6
Wen513	cap dolostone	82.0	1.07	25.75	14.15	0.34	0.0062	0.55	55.43	−2.6	−7.2
Wen522	chert	36.0	1.65	23.48	12.44	0.20	0.0094	0.53	21.25	−1.1	−4.8
Wen525	chert	18.0	1.20	28.31	14.20	0.34	0.0141	0.50	24.02	−0.4	−4.3
Wen534	dolostone	87.0	0.50	27.02	12.77	0.10	0.0146	0.47	6.78	3.6	−1.3
Son516	carbonate	89.7	0.23	38.57	0.21	0.05	0.0245	0.01	1.95	−9.3	−12.5
Son517	carbonate	75.6	1.17	22.88	10.27	0.11	0.0190	0.45	5.98	−7.4	−7.5
Son518	carbonate	89.1	0.17	38.55	0.19	0.04	0.0199	0.01	1.85	−9.2	−12.6
Son521	cap limestone	87.4	0.18	38.84	0.36	0.03	0.0223	0.01	1.49	−9	−13.1
Son564	limestone	84.6	1.08	37.65	0.43	0.04	0.4698	0.01	0.09	0.8	−11.3
Son572	limestone	18.3	3.78	25.63	1.35	0.12	0.9391	0.05	0.13	−1.6	−11.7
Son574	limestone	93.1	0.17	38.32	0.26	0.01	0.6085	0.01	0.01	2.3	−1.4
Son577	limestone	83.3	0.75	28.49	0.24	0.03	0.6903	0.01	0.04	0.1	−13
	min	6.5	0.1	16.7	0.1	0.0	0.0	0.00	0.0	−9.3	−13.1
	max	97.5	7.6	38.8	14.2	0.8	0.9	0.58	55.4	3.6	−1.3
	average	73.6	1.3	27.6	7.0	0.2	0.1	0.29	10.5	−3.2	−7.7

isotope data and will draw our conclusions about the carbon isotopic evolution on the basis of respective organic carbon isotope results.

7. Discussion

7.1. The Yanwutan–Lijiatuo section

Observed stratigraphic variations in carbon isotopic composition throughout the terminal Neoproterozoic and Early Cambrian sedimentary succession on the Yangtze Platform will be largely evaluated on respective data measured for organic carbon in samples from the Yanwutan–Lijiatuo section. Located in a slope to basinal setting, this section provides the most complete record for this study (Figs. 2 and 3). Results from the other sections described above will be compared to Yanwutan–Lijiatuo and discussed in respect to lateral, i.e. facies changes across the Yangtze Platform (Fig. 4).

Lithological changes up-section are clearly expressed by distinct variations of inorganic and organic carbon abundances (TIC, TOC in Tab. 4). Only carbonates in the lower 50 m of the Doushantuo Formation show TIC values above 0.1 wt.%. TOC abundances for the entire succession vary between 0.1 and 19.2 wt. % (average 3.8 ± 4.6 wt.%, $n = 134$) with the highest values measured for the Early Cambrian black shales of the Xiaoyanxi Formation.

The organic carbon isotope record is based on 126 samples (Fig. 3; Table 4), starting with post-glacial cap carbonates at the base and followed by dolostones of the Doushantuo Formation through the largely cherty Liuchapo Formation, across the Precambrian–Cambrian transition and well into the black shales of the Early Cambrian Xiaoyanxi Formation. A distinct shift from $\delta^{13}C_{org}$ values around −28.4‰ to a less negative value of −21.5‰ through the cap dolostone is followed by black shales and organic-rich dolostones with TOC
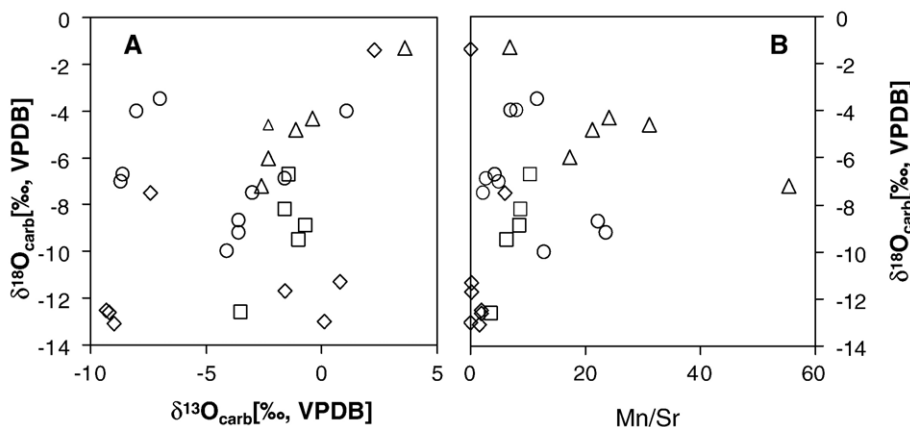
Fig. 5. Cross-plot of $\delta^{18}O_{carb}$ and $\delta^{13}C_{carb}$ (A) and $\delta^{18}O_{carb}$ and Mn/Sr (weight ratio) (B). Circles display values from the Yanwutan–Lijiatuo section, squares the Shatan section, diamonds the Songtao section and triangles the Weng'an section.

values of up 7.3 wt.% and displaying reasonably stable organic carbon isotope values between −32 and −30‰. These are followed by muddy to cherty dolostones with somewhat lower TOC abundances and strongly fluctuating $\delta^{13}C_{org}$ values from distinctly more negative (ca. −34‰) to mostly elevated values around −29‰. These carbon isotope oscillations occur within a proposed allochthonous slide sheet (see Vernhet et al., 2007-this volume), originating from the shallower part of the platform. Hence, carbon isotope variations reflect mixing of different proportions of autochtonous and resedimented organic material.

While there is no obvious correlation between TOC and $\delta^{13}C_{org}$, the strongly negative $\delta^{13}C$ values in the Doushantuo Formation likely reflect some contribution from bacterial biomass in addition to organic matter derived from primary production.

Towards the top of the Doushantuo Fm. and throughout the Liuchapo Fm., black shales and black cherts dominate with high abundances of TOC and relatively stable $\delta^{13}C_{org}$ values between −35 and −33‰.

An evolution towards less negative $\delta^{13}C_{org}$ values continues into the lower part of the Xiaoyanxi Formation with minimum values around −30‰. It is followed up-section by a distinct shift to rather stable and more negative $\delta^{13}C_{org}$ values between −34 and −33‰ in the upper 37 m of the Xiaoyanxi Formation. This suggests a clear change either in environmental conditions (such as a change in oxygenation of the water column) or in the type of organic material deposited in the sediment. While the organic carbon isotopic composition defines a clear stratigraphic trend, no distinct difference in TOC abundance across stratigraphy is discernible.

7.2. Comparison between different facies belts

As outlined above, the Yangtze Platform is characterized by distinct changes in depositional environments ranging from shallow shelf via slope into the deeper basin (e.g. Li et al., 1999a,b; Steiner et al., 2001; Jiang et al., 2003a,b; Shen et al., 2005). These define SW–NE trending facies belts. The sections studied here are located along a profile across these different facies belts. This allows the characterization of possible lateral changes in geochemical signatures related to facies variations across time-equivalent stratigraphic units (Figs. 1 and 2).

Organic and carbonate carbon isotope data for the postglacial Doushantuo Formation were obtained for samples from the Weng'an, Songtao and Yanwutan–Lijiatuo sections, representing a progressive deeping of the depositonal environment. Organic carbon isotope values ($\delta^{13}C_{org}$) for the Doushantuo Fm. at Weng'an range from −32.3 to −24.5‰ (average −28.1±2.5‰, $n=20$) and $\delta^{13}C_{carb}$ vary between −4.9 and +3.6‰ (average −1.1±2.0‰, $n=26$). The platform setting, and hence the carbon isotope data, are considered to reflect open ocean conditions. In contrast, both the organic and carbonate carbon isotopic records from Songtao section, although rather discontinuous, display comparatively more ^{13}C depleted values around an average of −33.7±2.2‰ ($n=7$) and −8.6±0.7‰ ($n=7$), respectively. It suggests the incorporation of some ^{13}C depleted bacterial biomass into the total sedimentary organic matter pool. Finally, large oscillations in the lower part of the Doushantuo Fm. at Yanwutan are confined to proposed mass flows from the platform. Geochemical results are distinctly different in

TOC and carbon isotopic composition from under-and overlying portions of the Doushantuo Formation. In part, they resemble respective values at Weng'an (Fig. 4).

The dolomitic and in part phosphoritic Doushantuo Formation is followed by massive light grey carbonates of the Dengying Formation on the carbonate platform and largely black cherts of the Liuchapo Formation in the deeper settings. The latter is well expressed in the basinal Yanwutan–Lijiatuo section but also at Songtao in the transition belt, however, in a much more condensed succession. Here, the organic carbon isotopic composition varies in a narrow range between −35.2 and −34.1‰ (average −34.5±0.3‰, n=11). This is quite comparable to the range in $\delta^{13}C_{org}$ observed for time-equivalent samples from the Yanwutan–Lijiatuo section. It suggests that comparable environmental conditions prevailed during that time in the transition and basin belts. Few samples from the uppermost Dengying Formation at the Shatan section display $\delta^{13}C_{org}$ values between −35.6 and −34.1‰ (n=5). The sediments exposed at the Shatan section were deposited under shallow water conditions and are represented by carbonates. Their carbonate carbon isotopic composition varies from −2.3 to 0.6‰ (n=14), yielding an average ε_{TOC} ($\delta^{13}C_{carb}$–$\delta^{13}C_{org}$) of 33.9±0.7‰ (n=5). Comparably high ε_{TOC} values>32‰ have been reported for several sections of late Neoproterozoic/Early Cambrian time (Hayes et al., 1999), and these high values are interpreted to reflect the incorporation of ^{13}C-depleted chemoautotrophic biomass to the total organic carbon.

The Early Cambrian on the Yangtze Platform is characterized by the widespread deposition of black shale, during a large scale transgressive event (the Niutitang event) which affected the entire platform. It is believed that at least the sediments from the lower part of the Early Cambrian succession (the Niutitang Formation and time-equivalent stratigraphic units) were deposited under anoxic bottom water conditions (Steiner, 2001; Goldberg et al., this volume).

The Early Cambrian black shale succession was studied at the Yanwutan–Lijiatuo, Songtao and Shatan sections. At all three locations, distinct stratigraphic variations in $\delta^{13}C_{org}$ occur. These are accompanied by clear variations in TOC abundance up-section at Shatan, less clear at Songtao and without any significant stratigraphic correlation at the Yanwutan–Lijiatuo section. It should be noted that TOC abundances are highest in the basinal Yanwutan–Lijiatuo section.

Despite low abundances in carbonate carbon (TIC), the carbonate carbon isotopic composition of black shale samples from the Guojiaba Formation at Shatan broadly parallels the organic carbon isotope record. This is expressed in largely invariable ε_{TOC} values between 30.5 and 32.9 ‰.

Based on abundances of organic carbon, biogenic sulphur and reactive Fe (see also Goldberg et al., 2007-this volume), the marked change in chemical/isotopic composition in the Early Cambrian black shale sequence is interpreted to reflect a change from decidedly anoxic to possibly dysoxic bottom water conditions. Sulphur isotope data for pyrite-and organically bound sulphur are consistent with this interpretation and indicate vertical fluctuations of a chemocline within the Early Cambrian water column on the Yangtze Platform. Higher TOC abundances and generally more negative $\delta^{13}C$ values for organic and carbonate carbon in the lower part of the Early Cambrian sedimentary sequence would be consistent with a higher deposition of organic matter and the anaerobic recycling of sedimentary organic matter. Resulting ^{13}C depleted DIC was obviously incorporated during carbonate formation in the coeval carbonate. The parallel trend in $\delta^{13}C_{org}$ and $\delta^{13}C_{carb}$ suggests that the DIC budget of the Early Cambrian water column (at least on the Yangtze Platform) was affected by anaerobic recycling of sedimentary organic matter and/or chemoautotrophy (cf. Hayes et al., 1999). The presence of pyrite and organically bound sulphur in these sediments indicates the activity of sulphate-reducing bacteria (Goldberg et al., 2007-this volume).

Up-section, TOC abundances decrease and $\delta^{13}C_{org}$ values become less negative at all three sections. Goldberg et al. (2007-this volume) interpret this shift as a change from anoxic to dysoxic/oxic which is supported by the degree of pyritization (DOP) as a proxy for bottom water oxygenation (e.g. Raiswell et al., 1988). Under this scenario, total sedimentary organic matter likely contains a smaller contribution of bacterial organic matter. Overall lower organic carbon abundances, but even more so less ^{13}C depleted organic carbon isotope values are consistent with this interpretation.

As noted above, the Yanwutan–Lijiatuo section continues further up and displays a shift back to more negative $\delta^{13}C_{org}$ values around −34‰ in the upper 37 m of the Xiaoyanxi Formation.

8. Conclusion

Temporal variations in the carbon isotopic composition exist across the studied time interval. In part, these likely reflect secular changes in organic carbon burial. In addition, however, variable bottom water redox conditions result in the incorporation of variable amounts of ^{13}C depleted bacterial biomass. Facies differences favoring this input (from platform to deeper water) seem to

disappear following the widespread Early Cambrian transgression and subsequent black shale deposition (Niutitang event). Results from this study reveal that caution must be placed on environmental issues prior to chemostratigraphic correlation.

Acknowledgements

References

Berner, R.A., 1981. A new geochemical classification of sedimentary environments. J. Sediment. Petrol. 51, 359–365.

Bowring, S.A., Grotzinger, J.P., Isachsen, C.E., Knoll, A.H., Pelechaty, S.M., Kolosov, P., 1993. Calibrating rates of Early Cambrian evolution. Science 261, 1293–1298.

Brasier, M.D., 1990a. Phosphogenic events and skeletal preservation across the Precambrian–Cambrian boundary interval. In: Notholt, A.J.G., Jarvis, I. (Eds.), Phosphorite Research and Development. Geol. Soc., Lond., Spec. Publ., vol. 52, pp. 282–303.

Brasier, M.D., 1990b. Nutrients in early Cambrian. Nature 347, 521–522.

Brasier, M.D., Magaritz, M., Corfield, R., Luo, H., Wu, X., Ouyang, L., Jiang, Z., Hamadi, B., He, T., Frazier, A.G., 1990. The carbon-and oxygen-isotopic record of the Precambrian–Cambrian boundary interval in China and Iran and their correlation. Geol. Mag. 127, 319–332.

Chu, X., Zhang, Q., Zhang, T., Feng, L., 2003. Sulphur and carbon isotopic variations in Neoproterozoic sedimentary rocks from southern China. Prog. Nat. Sci. 13 (11), 875–880.

Claypool, G.E., Kaplan, I.R., 1974. The origin and distribution of methane in marine sediments. In: Kaplan, I.R. (Ed.), In Natural Gases in Marine Sediments. Plenum Press, New York, pp. 99–139.

Condon, A., Zhu, M., Bowring, S., Wang, W., Yang, A., Jin, Y., 2005. U-Pb Ages from the Neoproterozoic Doushantuo Formation China. Science 308, 95–98.

Des Marais, D.J., 2001. Isotopic evolution of the Biogeochemical carbon cycle during the Precambrian. In: Valley, J.W., Cole, D.R. (Eds.), Stable Isotope Geochemistry (Reviews in Mineralogy and Geochemistry), vol. 43. Mineralogy Society of America, Washington, pp. 555–578.

Des Marais, D.J., Strauss, H., Summons, R.E., 1992. Carbon isotope evidence for the stepwise oxidation of the Proterozoic environment. Nature 359, 605–609.

Fu, J., Qin, K., 1995. Kerogen geochemistry. Guangdong Science and Technology Press, Guangzhou. 637 pp., (in Chinese).

Goldberg, T., Strauss, H., Guo, Q., Liu, C., 2007. Reconstructing marine redox conditions for the Early Cambrian Yangtze Platform: evidence from biogenic sulphur and organic carbon isotopes. Palaeogeography, Palaeoclimatology, Palaeoecology 254, 172–190 (this volume) , doi:10.1016/j.palaeo.2007.03.015.

Gradstein, F.M., Ogg, J.G., Smith, A.G., 2005. A Geologic Time Scale 2004. Cambridge University Press 0521786738.

Guo, Q., Liu, C., Strauss, H., Goldberg, T., 2003. Isotopic evolution of the terminal Neoproterozoic and early Cambrian carbon cycle on the northern Yangtze Platform, South China. Prog. Nat. Sci. 13 (12), 942–945.

Hayes, J.M., Kaplan, I.R., Wedeking, K.M., 1983. Precambrian organic geochemistry, preservation of the record. In: Schopf, J.W. (Ed.), Earth's Earliest Biosphere: Its Origin and Evolution. Princeton Univ. Press, Princeton, NJ, pp. 93–134.

Hayes, J.M., Strauss, H., Kaufman, A.J., 1999. The abundance of ^{13}C in Marine Organic matter and isotopic fractionation in the Global biogeochemical cycle of carbon during the past 800 Ma. Chem. Geol. 161, 103–125.

He, Y., Yang, X., 1986. Coelenterate fossils of the early-Early Cambrian from Nanjiang, Sichuan Province, China (in Chinese). Chengdu Institute of geological Mineral deposits publication. CAGS 7, 31–48.

Hoffman, P.F., Kaufman, A.J., Halverson, G.P., Schrag, D.P., 1998. A Neoproterozoic Snowball Earth. Science 281, 1342–1346.

Irwin, H., Curtis, C., Coleman, M., 1977. Isotopic evidence for source of diagenetic carbonates formed during burial of organic-rich sediments. Nature 269, 209–213.

Jacobsen, S.B., Kaufman, A.J., 1999. The Sr, C and O isotopic evolution of Neoproterozoic seawater. Chem. Geol. 161, 37–57.

Jiang, G., Kennedy, M.J., Christle-Blick, N., 2003a. Stable isotopic evidence for methane seeps in Neoproterozoic postglacial cap carbonates. Nature 426, 18–25.

Jiang, G., Sohl, L.E., Christie-Blick, N., 2003b. Neoproterozoic stratigraphic comparison of the Lesser Himalaya (India) and Yangtze block (South China): Paleogeographic implications. Geology 917–920.

Kaufman, A.J., Knoll, A.H., 1995. Neoproterozoic variations in the C-isotopic composition of seawater: Stratigraphic and biogeochemical implications. Precambrian Res. 73, 27–49.

Kaufman, A.J., Jacobsen, S.B., Knoll, A.H., 1993. The Vendian record of Sr-and C-isotopic variations in seawater: Implications for tectonic and paleoclimate. Earth Planet. Sci. Lett. 120, 409–430.

Kirschvink, J.L., Raub, T.D., 2003. A methane fuse for the Cambrian explosion: carbon cycles and true polar wander. C. R. Geoscience 335, 65–78.

Knoll, A.H., 1991. End of the Proterozoic Eon. Sci. Am. 265, 64–73.

Knoll, A.H., 1992. Biological and biogeochemical preludes to the Ediacaran radiation. In: Lipps, T.H., Signor, P.W. (Eds.), Origin and Early Evolution of Metazoans. Plenum Press, New York, pp. 53–84.

Knoll, A.H., 2000. Learning to tell Neoproterozoic time. Precambrian Res. 100, 3–20.

Knoll, A.H., Hayes, J.M., Kaufman, A.J., Swett, K., Lambert, I.B., 1986. Secular variation in carbon isotope ratios from upper Proterozoic successions of Svalbard and East Greenland. Nature 321, 832–838.

Kump, L.R., Arthur, M.A., 1999. Interpreting carbon-isotope excursions: carbonates and organic matter. Chem. Geol. 161, 181–198.

Lambert, I.B., Walter, M.R., Zang, W., Lu, S., Ma, G., 1987. Paleo-environment and carbon isotope stratigraphy of Upper Proterozoic carbonates of the Yangtze Platfrom. Nature 325, 140–142.

Lei, J., Li, R., Tobschall, H.J., Pu, Y., Fang, J., 2000. The characteristics of the sulphur species and their implications in lower Cambrian black shales from southern margin of Yangtze Platform. Sci. China, Ser. D: Earth Sci. 30 (6), 592–601.

Lewan, M.D., 1986. Stable carbon isotopes of amorphous kerogens from Phanerozoic sedimentary rocks. Geochim. Cosmochim. Acta 50, 1583–1591.

Li, C., Chen, J., Hua, T., 1998. Precambrian sponges with cellular structures. Science 279, 879–882.

Li, R., Lu, J., Zhang, S., Lei, J., 1999a. Organic carbon isotopes of the Sinian and Early Cambrian black shales on Yangtze Platform, China. Sci. China, Ser. D: Earth Sci. 42 (6), 595–603.

Li, R., Chen, J., Zhang, S., Lei, J., Shen, Y., Chu, X., 1999b. Spatial and temporal variations in carbon and sulphur isotopic compositions of Sinian sedimentary rocks in the Yangtze platform, South China. Precambrian Res. 97, 59–75.

Macouin, M., Besse, J., Ader, M., Gilder, S., Yang, Z., Sun, Z., Agrinier, P., 2004. Combined paleomagnetic and isotopic data from the Doushantuo carbonates, South China: implications for the "snow-ball Earth" hypothesis. Earth Planet. Sci. Lett. 224, 387–398.

Magaritz, M., Holser, W.T., Kirschvink, J.L., 1986. Carbon-isotope events across the Precambrian–Cambrian boundary on the Siberian Platform. Nature 320, 258–259.

Marshall, J.D., 1992. Climatic and oceanographic isotopic signals from the carbonate rock record and their preservation. Geol. Mag. 129, 143–160.

McCrea, J.M., 1950. On the isotopic chemistry of carbonates and a paleotemperture scale. Journal of Chemical Physics 18, 849–857.

Popp, B.N., Anderson, T.F., Sandberg, P.A., 1986. Textural, elemental and isotopic variations among constituents in Middle Devonian limestones, North America. J. Sediment. Petrol. 56, 27–715.

Raiswell, R., Buckley, F., Berner, R., Anderson, T., 1988. Degree of pyritization of iron as a paleoenvironmental indicator of bottom-water oxygenation. J. Sediment. Petrol. 58, 812–819.

Ripperdan, R.L., 1994. Global variations in carbon isotope composition during the latest Neoproterozoic and earliest Cambrian. Annu. Rev. Earth Planet. Sci. 22, 385–417.

Samuelsson, J., Strauss, H., 1999. Stable isotope geochemistry and paleobiology of the upper Visingsö Group (early Neoproterozoic), southern Sweden. Geol. Mag. 136, 63–73.

Shen, Y., 2002. C-isotope variations and paleoceanographic changes during the late Neoproterozoic on the Yangtze Platfrom, China. Precambrian Res. 113, 121–133.

Shen, Y., Schidlowski, M., 2000. New C isotope stratigraphy from southwest China: implications for the placement of the Precambrian–Cambrian boundary on the Yangtze Platform and global correlations. Geology 28, 623–626.

Shen, Y., Zhao, R., Chu, X., Lei, J., 1998. The carbon and sulphur isotope signatures in the Precambrian–Cambrian transition series of the Yangtze Platform. Precambrian Res. 89, 77–86.

Shen, Y., Schidlowski, M., Chu, X., 2000. Biogenchemical approach to understanding phosphogenic events of the terminal Proterozoic to Cambrian. Palaeogeogr. Palaeoclimatol. Palaeoecol. 158, 99–108.

Shen, Y., Zhang, T., Chu, X., 2005. C-isotopic stratification in a Neoproterozoic postglacial ocean. Precambrian Res. 137, 243–251.

Shields, G., Kimura, H., Yang, J., Gammon, P., 2004. Sulphur isotopic evolution of Neoproterozoic–Cambrian seawater: New francolite-bound sulphate $\delta^{34}S$ data and a critical appraisal of the existing record. Chem. Geol. 204, 163–182.

Steiner, M, 2001. Die fazielle Entwicklung und Fossilverbreitung auf der Yangtze Platform (Südchina) im Neoproterozoikum/frühsten Cambrian. Freiberger Forschungshefte. C 492, 1–26.

Steiner, M., Wallis, E., Erdtmann, B.D., Zhao, Y., Yang, R., 2001. Submarine- hydrothermal exhalative ore layers in black shales from South China and associated fossils — insights into a Lower Cambrian facies and bio-evolution. Palaeogeogr. Palaeoclimatol. Palaeoecol. 169, 165–191.

Steiner, M., Li, G., Qi, Y., Zhu, M., 2004. Lower Cambrian small shelly fossils of northern Shaanxi (China), and their biostratigraphic importance. Geobios 37, 259–275.

Strauss, H., 2004. 4 Ga of seawater evolution: Evidence from the sulphur isotopic composition of sulphate. In: Amend, J.P., Edwards, K.J., Lyons, T.W. (Eds.), In Sulphur Biogeochemistry—Past and Present, vol. 379. Geological Society of America, Boulder, pp. 195–205.

Strauss, H., Des Marais, D.J., Hayes, J.M., Summons, R.E., 1992a. Proterozoic organic carbon — its preservation and isotopic record. In: Schidlowski, M., Golubic, S., Kimberley, M.M., Mckirdy, D.M., Trudinger, P.A. (Eds.), In Early Organic Evolution: Implications for Mineral and Energy Resources. Springer Verlag, Berlin Heidelberg, pp. 203–211.

Strauss, H., Des Marais, D.J., Hayes, J.M., Summons, R.E, 1992b. Concentrations of organic carbon and maturities and elemental compositions of Kerogens. Cambridge University Press, United Kingdom, pp. 95–99.

Strauss, H., Des Marais, D.J., Hayes, J.M., Summons, R.E., 1992c. Abundances and isotopic compositions of carbon and sulphur species in whole rock and kerogen samples. In: Schopf, J.W., Klein, C. (Eds.), In the Proterozoic Biosphere — a Multidisciplinary Study. Cambridge University Press, Cambridge, pp. 711–798.

Veizer, J., 1983. Chemical diagenesis of carbonates: theory application. In: Arthur, M.A, et al. (Ed.), Stable Isotopes in Sedimentary Geology. Tulsa: S E P M Short Course, Soc. Econ. Palaeont. Mineral, vol. 10, p. 3-1-3-100.

Veizer, J., Bruckschen, P., Pawellek, F., Diener, A., Podlaha, O.G., Carden, G.A.F., Jasper, T., Korte, C., Strauss, H., Azmy, K., Ala, D., 1997. Oxygen isotope evolution of Phanerozoic seawater. Palaeogegr. Palaeoclimatol. Palaeoecol. 132, 159–172.

Veizer, J., Ala, D., Azmy, K., Bruckschen, P., Buhl, D., Bruhn, F., Carden, G.A.F., Diener, A, Ebneth, S., Godderis, Y., Jasper, T., Korte, C., Pawellek, F., Podlaha, O.G., Strauss, H., 1999. $^{87}Sr/^{86}Sr$, $\delta^{13}C$ and $\delta^{18}O$ evolution of Phanerozoic seawater. Chem. Geol. 161, 59–88.

Vernhet, E., Heubeck, C., Zhu, M., Zhang, J., 2007. Stratigraphic reconstruction of Yangtze Platfrom margin (Hunan Province, China) from shelf edge collapse products. Palaeogeography, Palaeoclimatology, Palaeoecology 254, 120–136 (this volume) , doi:10.1016/j. palaeo.2007.03.012.

Wachter, E.A., Hayes, J.M., 1985. Exchange of oxygen isotopes and carbon isotopes in carbon dioxide-phosphoric acid systems. Chem. Geol. 52, 365−74.

Walter, M.R., Veevers, J.J., Calver, C.R., Gorjan, P., Hill, A.C., 2000. Dating the 840–544Ma Neoproterozoic interval by isotopes of strontium, carbon, and sulphur in seawater, and some interpretative models. Precambrian Res. 100, 371–433.

Wang, Z., Yang, J., Sun, W., 1996. Carbon isotope record of Sinian seawater in Yangtze platform. Geol. J. Univ. 2 (1), 112–119.

Wu, C., 2000. Recovery of the paleoocean environment in the alternating epoch of late Sinian and early Cambrian in the west Hu'nan. Earth Sci. Front. 7, 45–57 (Suppl.).

Xiao, S., Zhang, Y., Knoll, A.H., 1998. Three-dimensional preservation of algae and animal embryos in a Neoprotoerozoic phosphorite. Nature 391, 553–558.

Yang, X., He, Y., 1984. New small shelly fossils genera of the Lower Cambrian from Nanjiang, Sichuan Province, China (in Chinese). Strata and paleontology papers assemblage, 13, pp. 35–47.

Yang, X., He, Y., Deng, S., 1983. Precambrian–Cambrian boundary and small shelly fossils fauna from Nanjiang, Sichuan Province, China (in Chinese). Chengdu Institute of geological Mineral deposits publication. CAGS 4, 91–110.

Yang, J., Sun, W., Wang, Z., Xue, Y., Tao, X., 1999. Variations in Sr and C isotopes and Ce anomalies in successions from China: evidence for the oxygenation of Neoproterozoic seawater? Precambrian Res. 93, 215–233.

Yang, A., Zhu, M., Zhang, J., Li, G., 2003. Early Cambrian eodiscoid trilobites of the Yangtze Platform and their stratigraphic implications. Prog. Nat. Sci. 13 (12), 861–866.

Zhang, J., Li, G., Zhou, C., Zhu, M., Yu, Z., 1997. Carbon isotope profiles and their correlation across the Neoproterozoic–Cambrian boundary interval on the Yangtze platform, China. Bull. Natl. Museum Nat. Sci. 10, 107–116.

Zhang, T., Chu, X., Zhang, Q., Feng, L., Huo, W., 2003. Variations of sulphur and carbon isotopes in seawater during the Doushantuo stage in late Neoproterozoic. Chin. Sci. Bull. 48 (13), 1375–1380.

Zhen, S., Zhen, S., Mo, Z., 1986. Geochemistry analysis of stable isotope. Beijing University Press, Beijing. 486 pp. (in Chinese).

Zhou, C., Zhang, J., Li, G., Yu, Z., 1997. Carbon and oxygen isotopic record of the early Cambrian from the Xiaotan section, Yunnan, South China. Sci. Geol. Sin. 32 (2), 201–211.

Zhou, C., Xue, Y., Zhang, J., 1998. Stratigraphy and sedimentary environment of the Upper Sinian Doushantuo Formation in Weng'an phosphorite deposit, Guizhou Province. J. Strat. 22 (4), 308–314.

Zhu, M., Zhang, J., Steiner, M., Yang, A., 2003. Sinian–Cambrian stratigraphic framework for shallow-to deep-water environments of the Yangtze Platform: an integrated approach. Prog. Nat. Sci. 13 (12), 951–960.